

ENC-2022-0215

NUMERICAL SIMULATION OF THE THERMOHYDRAULIC PERFORMANCE OF MWCNT/EG-WATER NANOFLUIDS IN AN AUTOMOTIVE RADIATOR

Erick Oliveira do Nascimento

Edwin Martin Cardenas Contreras

Enio Pedone Bandarra Filho

Federal University of Uberlândia (UFU), School of Mechanical Engineering, Av. Joao Naves de Ávila, 2121-Santa Monica, Uberlândia, MG 38400-902

erick.nascimento@ufu.br

emcardenas.1989@gmail.com

bandarra@ufu.br

Luben Cabezas-Gómez

Heat Transfer Research Group, São Carlos School of Engineering, University of São Paulo, Av. Trabalhador São-Carlense, 400, Pq Arnold Schmidt, CEP 13566-590 – São Carlos, SP, Brazil

lubengc@sc.usp.br

Abstract. Nanofluids are colloidal suspensions of nanometer-sized particles (less than 100 nm). This type of fluid has attracted attention for applications in heat transfer systems due to its higher thermal conductivity compared to base fluids such as ethylene glycol (EG) and water. The high cost of purchasing nanoparticles and the difficulty of preparing stable nanofluids is still one of the biggest obstacles of experimental methods, which makes computational fluid dynamics an important tool for predicting results. Thus, this work aims to simulate the convective heat transfer of the stationary laminar flow of MWCNT/Water-EG (50:50) nanofluids in a double row circular tube automotive radiator, with the software Ansys Fluent. Unlike most works, in which constant heat flux and temperature are considered at the wall, in this work, three computational domains were used (one for the air, another for the coolant and a third for the solid tube wall and fins regions). The liquid flow was numerically simulated for different nanofluid concentrations (0.25, 0.5 and 0.75 vol. %) in addition to the base fluid, under the condition that the solid particles are sufficiently dispersed to consider the fluid as single-phase and incompressible, for a mass flow of 0.09 – 0.11 kg/s and the nanofluid inlet temperature of 353.15 K. On the air side, the air velocity and temperature were kept constant at 2 m/s and 298.15 K, respectively, where the κ - ω SST model was applied to model the turbulence. It is also noteworthy that the thermophysical properties of the liquid are temperature dependent throughout the flow. This dependence was considered in the simulations through the implementation of a user-defined function (UDF). The results for the base fluid were compared with the results available in the literature and a maximum difference of less than 6% was observed in the prediction of the heat transfer rate. In addition, a tendency for the radiator outlet temperature to increase with the mass flow rate was identified, while the convective heat transfer coefficient increased about 15% with the nanofluid use. Therefore, from the results obtained, it can be said that nanofluids showed promising results for applications in automotive radiators, such as increasing the heat transfer rate of automotive radiators, which can be accomplished with the application of MWCNT nanoparticles.

Keywords: heat transfer, nanofluids, MWNCT, automotive radiator, computational fluid dynamics (CFD)

1. INTRODUCTION

In recent years, intensive research has been carried out on the thermal gains with the application of nanofluids (colloidal suspensions of nanometer-sized particles) compared to conventional fluids (such as water, ethylene glycol (EG) and a mixture of both). One of the most important promising applications of nanofluids is in the coolant of automotive radiators (Said et al., (2019) and Oliveira et al., 2021).

Naveen and Kishore (2020) experimentally evaluated the heat transfer of graphene/EG-water nanofluids for volumetric concentrations of 0.1 – 0.3% in an automotive radiator. In comparison with the base fluid, a maximum increase in the convective heat transfer coefficient of up to 68.04% was observed for the highest concentration and flow

rate. In addition, an increase in the Nusselt number of up to 53.4% was observed with the increase in flow rate and volumetric concentration of nanoparticles.

Devireddy et al. (2016) evaluated the behavior of the heat transfer coefficient of TiO_2/EG -water nanofluids compared to the base fluid for volumetric concentrations of 0.1 – 0.5% and in turbulent regime (4000 - 15000) in a radiator automotive. An increase of up to 37% in the heat transfer rate was observed.

Toh and Ting (2019) numerically studied the application of graphene/water nanoplate nanofluids in automotive radiators for the volumetric concentration of 0.5% in laminar regime. It was observed that the average Nusselt number increases with the concentration of nanoparticles and with the Reynolds number. For example, for the concentration of 0.5% and Reynolds 2000 number, an increase of 74.18% was identified.

Oliveira et al. (2017) evaluated the thermal performance of MWCNT/water nanofluids in an automotive radiator for different inlet temperatures (50 – 80 °C) and flow rate (30 – 70 g/s). It was observed that the heat transfer rate is dependent on the concentration of nanoparticles and on the inlet temperature. For example, for 80°C compared to 50°C, an increase of 180% was identified.

Contreras and Bandarra Filho (2022) experimentally investigated the thermal performance of multi-walled carbon nanotube (MWCNT)/EG-water nanofluids with volumetric concentrations of 0.025 – 0.1% in a double pass automotive radiator. On the air side, the inlet velocity and temperature were kept constant at 2 m/s and 25 °C, respectively, while the coolant had the mass flow rate and inlet temperature varying between 0.09 – 0.11 kg/s and 85 °C – 105 °C. Maximum increases of 4.6% and 4.4% were observed for the heat transfer rate and for the global heat transfer coefficient, respectively.

Thus, this work aims to numerically evaluate the thermohydraulic performance of MWCNT/EG-water (50:50) nanofluids in the automotive radiator experimentally analyzed by Contreras and Bandarra Filho (2022) for volumetric concentrations of 0.25 – 0.75 %, mass flow rate of 0.09 – 0.11 kg/s and inlet temperature of 353.15 K.

2. MATHEMATICAL DESCRIPTION AND GOVERNING EQUATIONS

2.1 Problem geometry

The automotive radiator analyzed in this work consists of 40 tubes with flat fins, distributed in two columns and divided into two passes. To simplify the problem, only one pair of tubes was simulated for each pass. As can be seen in Figure 1, four computational domains were created to model the problem, one for the tube wall, another for the air that flows over the tubes and between the fins, and two for the coolant. The geometric data of the equipment were obtained from the work of Contreras and Bandarra Filho (2022).

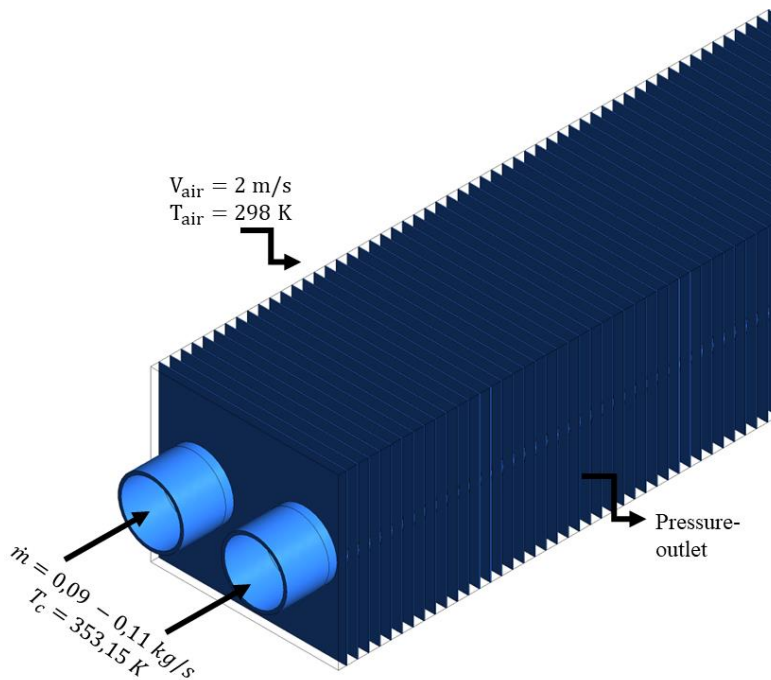


Figure 1. Problem geometry and boundary conditions.

Each tube has a length of 480 mm, an external diameter of 7 mm, with wall thickness of 0.35 mm. The fins are flat type with a thickness of 0.08 mm.

2.2 Governing equations

The coolant used in the simulations are the water-EG (50:50) and the MWCNT nanofluid with volumetric concentration between 0.25 – 0.75%. Due to the low volumetric concentration of nanoparticles, it was considered that the analyzed nanofluids are single-phase, Newtonian and incompressible. For all simulations, the internal fluid flows in a laminar regime, while the air side presents turbulent behavior, modeled by the κ - ω -SST model (the complete description of the model can be found in Menter (1993)). The equations of continuity (1), linear momentum (2) and energy (3) implemented in the Ansys Fluent software were used.

$$\frac{\partial(\rho_{\text{eff}}u_i)}{\partial x_i} = 0 \quad (1)$$

$$\frac{\partial}{\partial x_j}(\rho_{\text{eff}}u_i u_j) = -\frac{\partial p}{\partial x_i} + \frac{\partial}{\partial x_j} \left[\mu_{\text{eff}} \left(\frac{\partial u_i}{\partial x_j} + \frac{\partial u_j}{\partial x_i} - \frac{2}{3} \delta_{ij} \frac{\partial u_i}{\partial x_j} \right) \right] + \frac{\partial}{\partial x_j} (-\rho \overline{u_i' u_j'}) \quad (2)$$

$$\frac{\partial}{\partial x_i} [u_j(\rho_{\text{eff}}E + p)] = \frac{\partial}{\partial x_i} \left[\left(k_{\text{eff}} + \frac{C_p \mu_t}{Pr_t} \right) \frac{\partial T}{\partial x_j} + u_i (\tau_{ij})_{\text{eff}} \right] \quad (3)$$

where ρ_{eff} refers to the density, u_i is the velocity vector component, p is the pressure, μ_{eff} is the dynamic viscosity, C_p is the specific heat, T is the temperature, δ_{ij} is the Kronecker delta, $E = c_p T - (p/\rho) + (u^2/2)$ is the total energy and $(\tau_{ij})_{\text{eff}} = \left[\mu_{\text{eff}} \left(\frac{\partial u_j}{\partial x_i} + \frac{\partial u_i}{\partial x_j} \right) - \frac{2}{3} \mu_{\text{eff}} \frac{\partial u_i}{\partial x_j} \delta_{ij} \right]$ is the deviatoric stress tensor (Manca et al., 2012). It is noteworthy that the turbulence terms are used only for the air domain.

The energy equation for solid is described in Eq. (4).

$$\frac{\partial}{\partial x_i} \left(k \frac{\partial T}{\partial x_i} \right) = 0 \quad (4)$$

2.3 Numerical method

Equations (1 - 3) were solved using the finite volume method implemented in the Ansys Fluent software with double precision for all cases. The employed pressure-velocity coupling method was COUPLED and for the discretization of the convective and diffusive terms the second order upwind method was used.

2.4 Boundary conditions

As mentioned earlier, to reduce the computational cost, the computational model was reduced to one pair of tubes for each pass of the actual radiator. On the internal fluid side, a mass flow rate of 0.09 – 0.11 kg/s divided by the number of tubes of each pass was configured at the inlet, and inlet temperature fixed at 353.15 K, while on the air side, a speed of 2 m/s and a fixed temperature of 25 °C were defined at the inlet. On both sides, the output was configured as a pressure-outlet, see Figure 1.

2.5 Thermophysical properties

Throughout the flow, the properties of the base fluid are defined as a function of the local temperature, while the properties of the nanofluids were calculated through the correlation (5) for density, (6) for the dynamic viscosity, (7) for the thermal conductivity and (8) for the specific heat.

$$\rho_{\text{eff}}(T) = \phi \cdot \rho_{\text{np}} + (1 - \phi) \cdot \rho_{\text{bf}}(T) \quad (5)$$

$$\mu_{\text{eff}}(T) = \frac{\mu_{\text{bf}}(T)}{(1 - \phi)^{2.5}} \quad (6)$$

$$k_{\text{eff}}(T) = k_{\text{bf}}(T) \cdot \left(\frac{3 + \phi \cdot \frac{k_{\text{np}}}{k_{\text{bf}}(T)}}{3 - 2 \cdot \phi} \right) \quad (7)$$

$$(\rho \cdot C_p)_{\text{eff}}(T) = \phi \cdot (\rho \cdot C_p)_{\text{np}} + (1 - \phi) \cdot (\rho \cdot C_p)_{\text{bf}}(T) \quad (8)$$

2.6 Data reduction

The heat transfer rate was calculated through Eq. (9):

$$Q = \dot{m} \cdot C_{p_{\text{eff}}} \cdot (T_{\text{in}} - T_{\text{out}}) \quad (9)$$

where \dot{m} represents the mass flow rate, $C_{p_{\text{eff}}}$ refers to the specific heat of the nanofluid, T_{in} is the inlet temperature (353.15 K) and T_{out} is the nanofluid temperature at the outlet.

The local and average convective heat transfer coefficients are obtained through Eq. (10) and (11) respectively.

$$h_z = \frac{q''}{(T_w - T_f)_z} \quad (10)$$

$$h_{\text{avg}} = \frac{1}{L} \int_0^L h_z dz \quad (11)$$

where L , refers to the total length of the tube, T_w refers to the wall temperature, T_f is the fluid temperature and q'' is the heat flux.

The thermohydraulic performance coefficient is calculated through Eq. (12).

$$\eta = \frac{Q_{\text{nf}}/Q_{\text{bf}}}{\Delta p_{\text{nf}}/\Delta p_{\text{bf}}} \quad (12)$$

where Δp refers to the pressure drop. Subscripts bf and nf refer to base fluid and nanofluid.

3. GRID INDEPENDENCE STUDY

To perform the mesh independence study, simulations were performed for three meshes with different element sizes. Meshes with 2522074, 3278696 and 4262305 elements were used and the coolant outlet temperature was chosen as the solution convergence criterion.

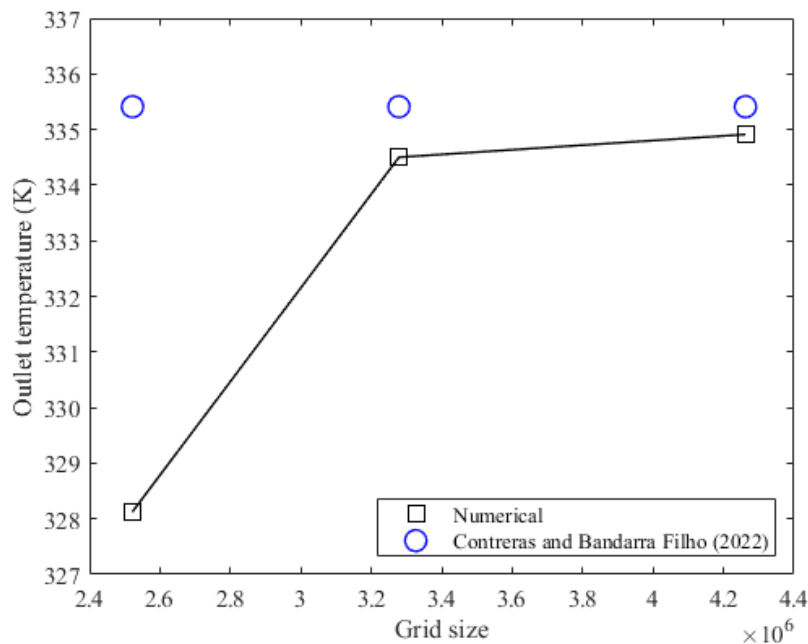


Figure 2. Grid independence study.

As can be seen in Figure 2, for the mesh with the smallest number of elements, the difference between the numerical result and the experimental one by Contreras and Bandarra Filho (2022) is 7.28 K, while for the second mesh there is a variation of only 0.91 K. The simulation with the mesh with the largest number of elements presented the closest result to the experimental results, however, the difference for the second mesh is only 0.12%, not justifying the computational increase. Thus, all the results presented in this work correspond to the simulations carried out with mesh 2.

4. RESULTS AND DISCUSSIONS

4.1 Heat transfer rate

Figure 3 illustrates the experimental heat transfer rate values for the base fluid and, the nanofluid with a concentration of 0.1 vol.% obtained by Contreras and Bandarra Filho (2022) and of the numerical simulated values for the base fluid and the nanofluids for concentrations of 0.25, 0.5 and 0.75 vol.%. It can be observed for the base fluid that the numerical results follow the prediction obtained experimentally, with an average difference of 4.16% for all the flows analyzed.

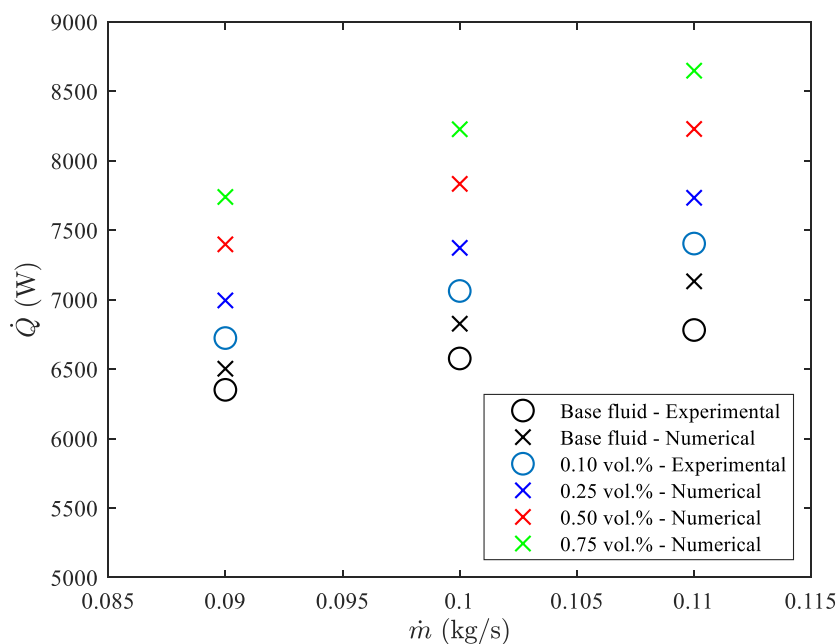


Figure 3. Heat transfer rate as a function of mass flow rate.

Contreras and Bandarra Filho (2022) obtained gains of up to 4.6% in relation to the base fluid for a volumetric concentration of 0.1% at a temperature of 353.15 K, while in this work maximum increases of 8.43%, 15.38% and 21.26% for volumetric concentrations of 0.25, 0.5 and 0.75 vol.%, respectively, were observed. In addition, the increase in the mass flow rate provided an increase in the heat transfer rate by up to 11.74% for the sample with a volumetric concentration of 0.75%.

4.2 Average heat transfer coefficient

Figure 4 shows the average heat transfer convective coefficient for the coolant as a function of the mass flow rate and the volumetric concentration of MWCNT nanoparticles for the first and second pass of the radiator. It can be observed that the increase in the flow rate and the insertion of nanoparticles provided an increase in the convective heat transfer coefficient in the two steps.

The increment of nanoparticles provided the maximum increase in the convective coefficient of 30.56% and 16.17% in the second pass. In pass 1 the gains are more pronounced compared to pass 2. This is due to the fact that in the first pass the fluid has higher thermal conductivity due to higher temperature. Still in Figure 4, it can be seen that the average convective coefficient tends to increase with the increase of the mass flow. Increases of up to 15.58% were observed for the volumetric concentration of 0.75%.

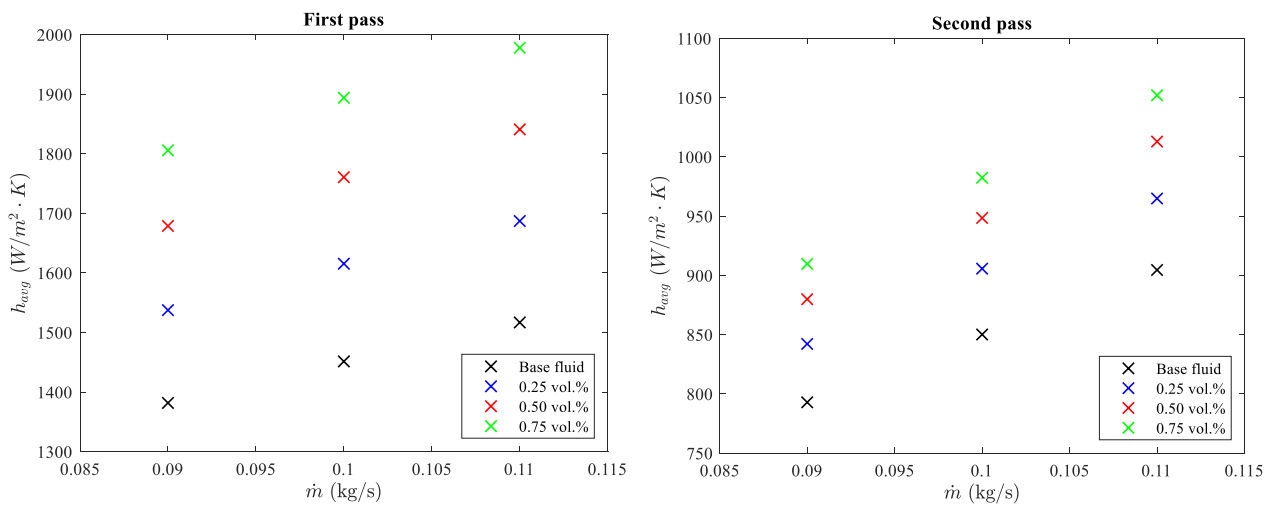


Figure 4. Heat transfer rate as a function of mass flow.

4.3 Pressure drop

As expected, it can be seen in Figure 5 that the increment of nanoparticles caused an increase in the pressure drop compared to the base fluid for all mass flow rates analyzed. For the highest concentration, an increase of up to 9.53% was observed in relation to the base fluid.

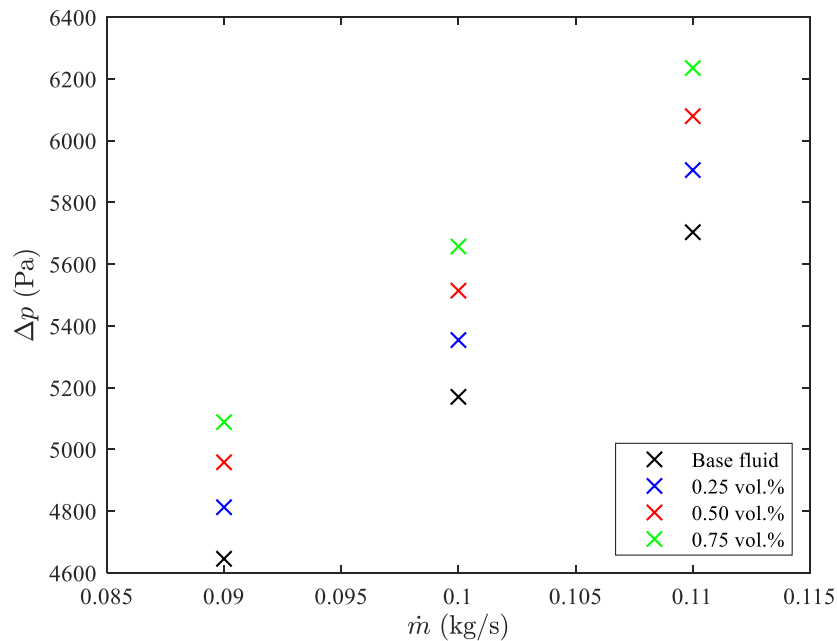


Figure 5. Pressure drop as a function of mass flow.

In addition, an increase in pressure drop was also observed as a function of the increase in mass flow rate, whose maximum value was 22.73%. Although stability was not considered in this work, it should be noted that when the nanofluid is subjected to the cooling process, it can lead to agglomeration of nanoparticles, causing a considerable increase in the pressure drop.

4.4 Thermohydraulic performance coefficient

The thermohydraulic Performance Coefficient (TPC) consists of the ratio of the gains in the heat transfer rate and the gains in the pressure drop of the nanofluids, according to Eq. (12). As can be seen in Figure 6, all analyzed nanofluids present TPC greater than 1. This means, that the gains in heat transfer are greater than the increase in pressure drop for all cases analyzed.

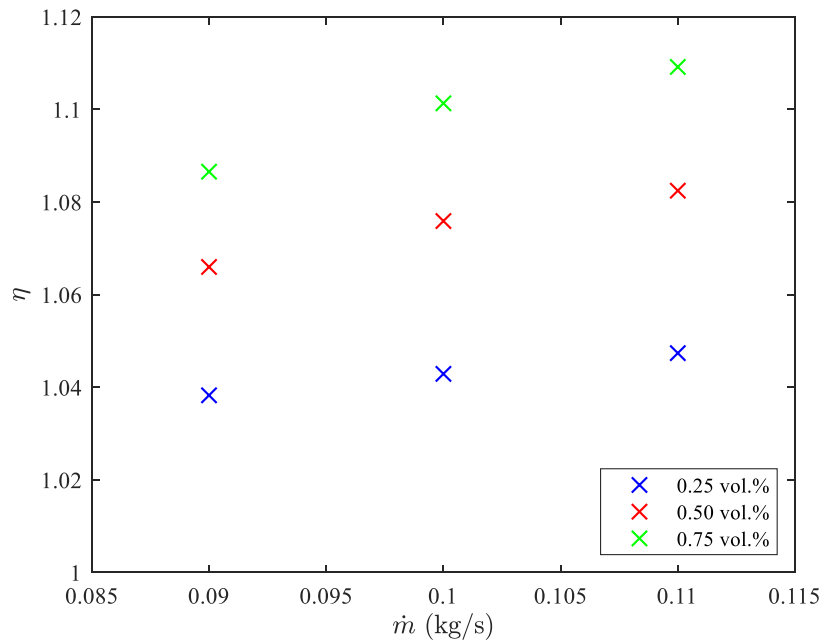


Figure 6. Thermohydraulic performance of the nanofluids analyzed.

Still in Figure 6, it can be seen that the thermohydraulic performance coefficient increases with the mass flow rate augmentation for all concentrations of MWCNT nanoparticles. The highest TPC value was 1.11 for a volumetric concentration of 0.75% and a mass flow rate of 0.11 kg/s. It should be noted that in this work, the possible effects of agglomeration and sedimentation of nanoparticles are not considered due to the considerable increase in nanoparticles, whose effect can reduce the thermal gains and increase the pressure drop, impairing the TPC value.

5. CONCLUSIONS

Computational modeling of the flow and heat transfer of MWCNT/water-EG nanofluids in a double pass automotive radiator in laminar regime was performed. The effect of temperature on the properties of the coolant, the increase in the mass flow rate and the volumetric concentration of nanoparticles was considered. The main conclusions obtained are highlighted below:

- There was an increase in the heat transfer rate due to the insertion of MWCNT nanoparticles of 21.26% and with the increase in the mass flow of 11.74%.
- The convective heat transfer coefficient increased by up to 30.56% for the nanofluid with the volumetric concentration of 0.75%.
- The addition of nanoparticles increased the pressure drop by up to 9.53% for a volumetric concentration of 0.75%.
- The thermohydraulic performance coefficient of the nanofluids was greater than 1 for all cases analyzed, which indicates a promising result for applications in automotive radiators. The highest TPC value was 1.11 for a mass flow of 0.11 kg/s and volumetric concentration of 0.75%.

Therefore, from a numerical point of view, the application of MWCNT/water-EG nanofluids analyzed in this work, show promising results for application in automotive radiators.

6. ACKNOWLEDGEMENTS

The authors are grateful for the financial support provided for this research by CNPq and FAPEMIG. The authors also wish to extend their gratitude to FCA, FIAT CHRYSLER AUTOMOVEIS BRASIL LTDA.

This study was financed in part by the Coordenação de Aperfeiçoamento de Pessoal de Nível Superior - Brasil (CAPES) - Finance Code 001

7. REFERENCES

- Naveen, N.S. and Kishore, P.S., 2020. "Experimental investigation on heat transfer parameters of an automotive car radiator using graphene/water-ethylene glycol coolant". *Journal of Dispersion Science and Technology*, Vol. 43, No. 3, pp. 1-13.
- Toh, L.K.L.; Ting, T.W., 2019. "Thermal performance of automotive radiator with graphene nanoplatelets suspension". *Aip Conference Proceedings*.
- Contreras, Edwin M.C.; Bandarra Filho, E.P., 2022. "Heat transfer performance of an automotive radiator with MWCNT nanofluid cooling in a high operating temperature range". *Applied Thermal Engineering*, Vol. 207, pp. 118149.
- Oliveira, G.A., Contreras, E.M.C. and Bandarra Filho, E.P., 2021. "Experimental study of thermophysical properties of MWCNT and graphene coolant nanofluids for automotive application". *Journal of the Brazilian Society of Mechanical Sciences and Engineering*, Vol. 43.
- Oliveira, G.A., Contreras, E.M.C. and Bandarra Filho, E.P., 2017. "Experimental study on the heat transfer of MWCNT/water nanofluid flowing in a car radiator". *Applied Thermal Engineering*, Vol. 111, pp. 1450-1456.
- Devireddy, S., Mekala, C.S.R. and Veeredhi, V.R., 2016. "Improving the cooling performance of automobile radiator with ethylene glycol water based TiO₂ nanofluids". *International Communications in Heat and Mass Transfer*, Vol. 78, pp. 121-126.
- Manca, O.; Nardini, S.; Ricci, D., 2012. "A numerical study of nanofluid forced convection in ribbed channels". *Applied Thermal Engineering*, Vol. 37, pp. 280-292.
- Menter, F., 1993. "Zonal Two Equation k-w Turbulence Models for Aerodynamic Flows". *23Rd Fluid Dynamics, Plasmadynamics, and Lasers Conference*.
- Said, Z.; Assad, M.E.H.; Hachicha, A.A.; Bellos, E.; Abdelkareem, M.A.; Alazaizeh, D.Z.; Yousef, B.A.A., 2019. "Enhancing the performance of automotive radiators using nanofluids". *Renewable And Sustainable Energy Reviews*, Vol. 112, pp. 183-194.

8. RESPONSIBILITY NOTICE

The author(s) is (are) the only responsible for the printed material included in this paper.